

Diffusion Disambiguation Models for Partial Label Learning

Jinfu Fan, *Member, IEEE* Xiaohui Zhong, Kangrui Ren, Jiangnan Li, Linqing Huang*, *Member, IEEE*,

Abstract—Learning from ambiguous labels is a long-standing problem in practical machine learning applications. The purpose of *partial label learning* (PLL) is to identify the ground-truth label from a set of candidate labels associated with a given instance. Inspired by the remarkable performance of diffusion models in various generation tasks, this paper explores their potential to denoise ambiguous labels through the reverse denoising process. Therefore, this paper reformulates the label disambiguation problem from the perspective of generative models, where labels are generated by iteratively refining initial random guesses. This perspective enables the diffusion model to learn how label information is generated stochastically. By modeling the generation uncertainty, we can use the maximum likelihood estimate of the label for classification inference. However, such ambiguous labels lead to a mismatch between instance and label, which reduces the quality of generated data. To address this issue, this paper proposes a *diffusion disambiguation model for PLL* (DDMP), which first uses the potential complementary information between instances and labels to construct pseudo-clean labels for initial diffusion training. Furthermore, a transition-aware matrix is introduced to estimate the potential ground-truth labels, which are dynamically updated during the diffusion generation. During training, the ground-truth label is progressively refined, improving the classifier. Experiments show the advantage of the DDMP and its suitability for PLL.

Index Terms—diffusion disambiguation model, partial label learning, transition-aware matrix.

I. INTRODUCTION

Supervised learning has achieved remarkable accuracy in various classification tasks, but it typically requires large amounts of labeled data. Nonetheless, large-scale data annotation is often costly and labor-intensive, yet the labeled data often suffers from inherent inaccuracies stemming from either human mistakes or limitations in algorithmic labeling approaches. Additionally, research has shown that learning with ambiguous labels can cause models to overfit the noisy labels, reducing their generalization ability [1]. Therefore, it is essential to leverage *partial label learning* (PLL) algorithms to effectively utilize cheap yet imperfect datasets for supervised learning tasks [2] [3]. PLL is a form of weakly supervised learning in which each training instance is associated with a set of possible labels, but only one of them represents the



Fig. 1. An example of partial label learning with noisy labels.

true label. PLL arises in many real-world scenarios such as image annotation (as shown in Figure 1), object detection, web mining, etc [4] [5]. In such scenarios, the primary difficulty lies in accurately pinpointing the ground-truth label from the set of candidate labels.

To mitigate the impact of ambiguous labels, two general machine learning strategies have been proposed, i.e. *non-deep learning strategy* (NDLS) [6] [7] [8] and *deep learning strategy* (DLS) [9] [10] [11]. NDLS employs various optimization techniques to iteratively refine label confidence, aiming to identify the ground-truth labels from the candidate label set. In contrast, DLS incorporates some training objectives compatible with stochastic optimization, such as adding regularization terms, data augmentation, and adjusting loss weight. However, the drawback of the above methods is that they overly rely on observations of similar instances to estimate the uncertainty of labels, which can lead to incorrect disambiguation of uncertain labels in negative nearest neighbor instances. Negative nearest neighbor usually refers to the nearest neighbor of the opposite class to the current instance, which includes instances with similar features but not the same labeled class among the k -nearest neighbors calculated by instance features. Such inaccuracies progressively build up and persistently influence the learning process of the model, ultimately constraining its effectiveness in partial label learning scenarios.

To tackle this issue, a novel *diffusion disambiguation model for PLL* (DDMP) is proposed. To alleviate the incorrect disambiguation caused by reliance on instance representation, this paper hopes to disambiguate candidate labels by learning the generation process of ambiguous labels, which naturally provides new insights into solving the PLL problem. Inspired by the remarkable performance of diffusion models [12] [13] in various generation tasks, this paper explores their potential

Jinfu Fan, Xiaohui Zhong and Jiangnan Li are with the College of Computer Science and Technology, Qingdao University, Qingdao, 266071, China.(E-mail:fan_jinfu@163.com, zhongxiaohui@qdu.edu.cn, li-jiangnan@qdu.edu.cn). Kangrui Ren is with the Department of Control Science and Engineering, College of Electronics and Information Engineering, Tongji University, Shanghai 201804, China (e-mail: 2310213@tongji.edu.cn). Linqing Huang is with the School of Electronic Information and Electrical Engineering, Shanghai Jiao Tong University, Shanghai 200240, China.(huanglinqing95@gmail.com).

to denoise ambiguous labels through the reverse denoising process. But to the best of our knowledge, there is no theoretical discussion and research on the diffusion model in PLL learning. Recently, *Classification and Regression Diffusion Models* (CARD) [14] have extended diffusion models to address classification and regression problems. Inspired by CARD, DDMP addresses ambiguous label learning by treating it as a random process where labels are conditionally generated via diffusion mechanisms, the challenge of ambiguous label learning is approached as a stochastic label diffusion process conditioned on instance features. DDMP consists of a forward process and a reverse process. In the forward process, we start to make noisy estimates of the ambiguous labels and then gradually reconstruct them to learn to recover the ground-truth labels as output, which is essentially the same as the reverse denoising step in a diffusion model. ***This task presents a significant challenge due to the presence of ambiguous labels. When training a diffusion model on a dataset with ambiguous labels, the model learns the conditional score associated with noisy labels.***

To reduce the ambiguity of candidate labels, a smoothness assumption can be adopted, that is similar instances are more likely to have the same label. To quantify label similarity, the Jaccard distance is used to compute a label similarity matrix, enabling deeper exploration of relationships between candidate labels. For instance relations, especially negative nearest neighbor instances, the label adjacency matrix can mitigate the impact of similar instances with different labels and avoid the output of an instance being overwhelmed by the output of its negative nearest instance. Therefore, we leverage the potential complementary information between instances and labels to construct pseudo-clean labels that can preliminarily alleviate the impact of ambiguous labels during diffusion model training. Furthermore, a transition-aware matrix is introduced to estimate the potential ground-truth labels, which are dynamically updated during the diffusion generation. Meanwhile, we theoretically prove the mutual enhancement between the pseudo-clean label matrix and the transition-aware matrix from the perspective of the *Expectation-Maximization* (EM) algorithm. In addition, as shown in Figure 2, this paper designs a diffusion model structure suitable for PLL, which instance guided cross attention and label guided cross attention are beneficial for the model to fully explore the potential effective information between instances and labels, and perform feature fusion to guide the model in learning how to denoise. Meanwhile, DDMP includes a flexible conditional injection mechanism that supports time steps to guide model learning, enabling the model to effectively learn complex functions that map from noisy labels to disambiguation labels. The forward denoising and reverse disambiguation processes iteratively improve performance, progressively refining ground-truth labels. These refined labels in turn help to enhance classifier training. In summary, the contributions of this paper are as follows:

- A novel *diffusion disambiguation model for PLL* (DDMP) is proposed, which reframes learning from ambiguous labels as a stochastic process of conditional label generation, enabling effective learning from data with am-

biguous labels.

- The pseudo-clean label matrix is redesigned based on information complementarity, leveraging the potential interactions between instances and labels to prevent the output of an instance from being overwhelmed by its nearest negative instance.
- An adaptive estimator strategy with a transition-aware matrix is proposed to correct ambiguous labels, with a theoretical foundation based on the EM perspective.

Comprehensive experiments validate the robustness and effectiveness of DDMP, showing its performance surpasses that of state-of-the-art methods on partial label datasets.

II. RELATED WORK

A. Partial Label Learning

Existing PLL algorithms fall into two main categories, i.e., *deep learning strategy* (DLS) and *non-deep learning strategy* (NDLS).

1) Non-deep Learning Strategy:

NDLS is built on the assumption that similar instances are likely to share the same label, and it resolves label ambiguity by exploring the underlying relationships between the candidate labels of similar instances. Various machine learning techniques, including *Expectation Maximization* (EM) [6] [15], *K-Nearest Neighbors* (KNN) [7] [16], *Support Vector Machine* (SVM) [8] [17] and *Low-Rank Representation* (LRR) [18] [19], have been widely applied to address PLL challenges. In addition, Zhang et al. [8] further deepened the mining of inter-label relationships by constructing a weighted graph and utilizing affinity analysis to achieve iterative propagation of label information and effective differentiation of ground-truth label. Fan et al. [20] proposed a competitive disambiguation strategy to reduce the influence of label ambiguity by updating the cluster center through competitive weighted disambiguation of neighboring instances. Wang et al. [3] introduced a discrimination enhancement strategy for PLL to improve label confidence by reinforcing discriminative features in the representation space.

However, the time complexity of most NDLS algorithms grows significantly with larger datasets. To address this limitation, an increasing number of researchers are turning to deep learning approaches to tackle the PLL problem.

2) Deep Learning Strategy:

The advancement of deep neural networks has spurred extensive research into establishing a deep learning framework for PLL. Yao et al. [9] pioneered the integration of PLL with deep learning by employing temporal coding techniques to combine outputs across different periods, guiding subsequent predictions. In the same year, Yao et al. [10] enhanced label disambiguation in network interactions through a cooperative network mechanism. Lv et al. [21] introduce a progressive recognition algorithm that iteratively refines ground-truth labels as the model evolves, ensuring strong compatibility. Wen et al. [22] incorporate a leverage parameter into the loss function, demonstrating promising experimental results across various deep learning frameworks. Besides, Fan et al. [23] integrated graph representation learning into the PLL problem,

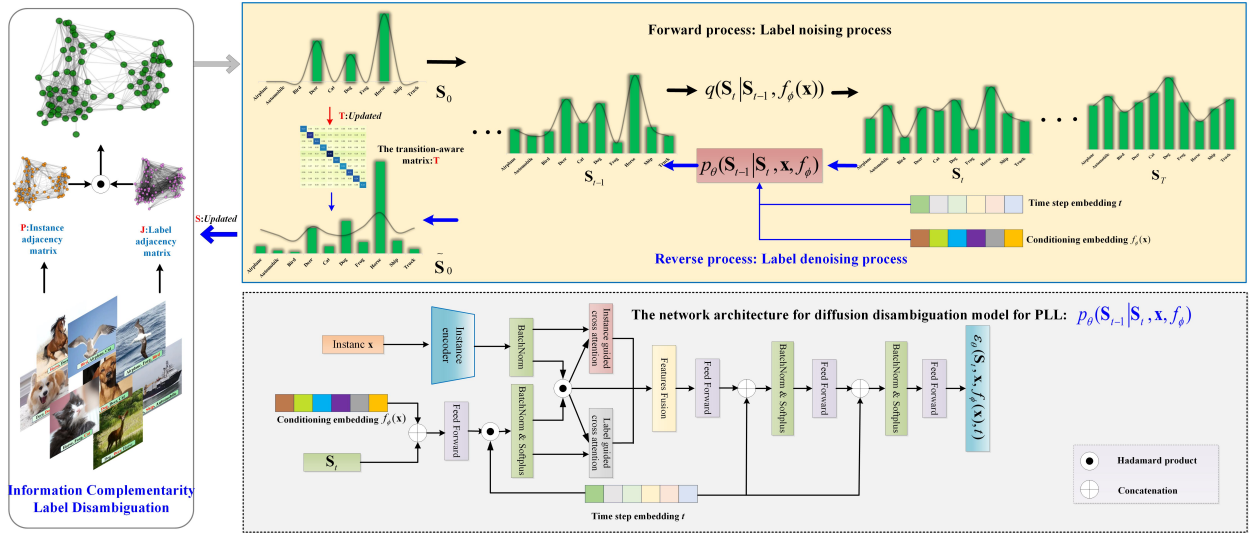


Fig. 2. The training procedure of the proposed DDMP approach.

developing a disambiguation correction network that significantly improved model performance in complex PLL scenarios by iteratively refining the disambiguation and correction processes. Subsequently, [11] extended graph neural networks to PLL by employing mutual information maximization for deeper representation-based partial label disambiguation. More recently, Wang et al. [24] introduced contrastive learning to PLL, leveraging the Momentum Contrast strategy to greatly enhance the representation learning ability of model. Additionally, Fan et al. [25] proposed a K-means cross-attention transformer for PLL, enabling continuous learning of cluster centers for effective disambiguation tasks. Realistically, instance-dependent partial label learning emerges as a more realistic framework for handling ambiguous supervision scenarios. To address this challenge, a series of methods like contrastive learning, bayesian models and variational inference have been proposed for instance dependent partial label learning [26]–[29].

One possible drawback of DLS is that it depends heavily on the relationships among candidate labels of similar instances, making it vulnerable to the influence of misleading or negative neighbor instances.

B. Diffusion Model

Generative models represent a crucial category of models in the realm of computer vision, and the diffusion model (DDPM) [12] [30] is very popular nowadays compared to VAE [31] and GAN [32]. Diffusion models are inspired by the diffusion phenomenon in physics, where particles migrate from areas of higher concentration to areas of lower concentration. In the context of machine learning, this idea is harnessed for data synthesis by first applying a forward process that incrementally corrupts data with noise, and then training a reverse process that learns to remove that noise to recreate clean samples. During training, the objective of the model is to estimate the exact noise added at each forward step, and those estimates are then used in the reverse (denoising) process to generate

new data. To speed up the sampling process, DDIM [33] has emerged, which can be accelerated by skipping steps. CARD [14] extends the diffusion model to the domain of classification and regression, which can be used to solve the labeling problem.

However, when the diffusion model faces ambiguous labeling, it presents a significant challenge for the reverse denoising process. During training on datasets with ambiguous labels, the model learns the conditional scores associated with noisy labels, which significantly reduces the performance of the model.

III. DDMP METHOD

A. Problem Formulation

This section formulates the problem of PLL. We define the feature space as $\mathcal{X} \in \mathbb{R}^d$ and the output space as $\mathcal{Y} = \{y_c : c = 1, \dots, Q\}$, where d is the feature dimension and Q is the number of classes. The training set for PLL is $\mathcal{D} = \{(\mathbf{x}_i, S_i) | 1 \leq i \leq N\}$, where $\mathbf{x}_i \subseteq \mathcal{X}$ represents instance features and $S_i \subseteq \mathcal{Y}$ represents the candidate label set associated with \mathbf{x}_i . Particularly, $|S_i|$ represents the number of ambiguous labels for instance \mathbf{x}_i . Meanwhile, the label confidence matrix can be denoted as $\mathbf{Y} = [\mathbf{y}_1, \mathbf{y}_2, \dots, \mathbf{y}_N]^T \in \mathbb{R}^{N \times Q}$, where each $\mathbf{y}_i \in \{0, 1\}^Q$ marks its candidate labels with 1 (and non-candidates with 0). The aim of DDMP is then to learn a classifier $\mathbf{f} : \mathcal{X} \mapsto \mathcal{Y}$ that can correctly predict labels for previously unseen inputs.

B. The Forward Process of DDMP

Much like in traditional diffusion frameworks [12], [34], DDMP is built around a forward and a reverse pass. During forward diffusion, the Q -dimensional pseudo-clean label S_0 undergoes progressive corruption across T timesteps, yielding intermediate states $S_{1:T}$. This converges asymptotically to $\mathcal{N}(f_\phi(\mathbf{x}), \mathbf{I})$ (latent distribution), where the mean f_ϕ comes from a pre-trained instance encoder, encoding prior information about the relationship between \mathbf{x} and S_0 . The initial

pseudo-clean label \mathbf{S} is calculated based on complementary information between instances and candidate labels, and is continuously updated during subsequent iterations, which will be described in detail later. The forward process in diffusion models, denoted as $q(\mathbf{S}_{1:T}|\mathbf{S}_0, f_\phi(\mathbf{x}))$, is also a Markov chain. It is defined by adding Gaussian noise to the data over time, and the form of the forward process conditional distributions in a similar fashion as [35], which can be summarized as follows:

$$q(\mathbf{S}_{1:T}|\mathbf{S}_0, f_\phi(\mathbf{x})) = \prod_{t=1}^T q(\mathbf{S}_t|\mathbf{S}_{t-1}, f_\phi(\mathbf{x})) \quad (1)$$

$$q(\mathbf{S}_t | \mathbf{S}_{t-1}, f_\phi(\mathbf{x})) = \mathcal{N}\left(\mathbf{S}_t; \sqrt{1 - \beta_t}\mathbf{S}_{t-1} + \left(1 - \sqrt{1 - \beta_t}\right) f_\phi(\mathbf{x}), \beta_t \mathbf{I}\right) \quad (2)$$

where $\{\beta_t\}_{t=1:T} \in (0, 1)^T$ is the variance schedule. This recursive formulation allows direct sampling of \mathbf{S}_t , with t an arbitrary timestep,

$$q(\mathbf{S}_t | \mathbf{S}_0, f_\phi(\mathbf{x})) = \mathcal{N}\left(\mathbf{S}_t; \sqrt{\bar{\alpha}_t}\mathbf{S}_0 + (1 - \sqrt{\bar{\alpha}_t}) f_\phi(\mathbf{x}), (1 - \bar{\alpha}_t)\mathbf{I}\right) \quad (3)$$

where $\alpha_t = 1 - \beta_t$ and $\bar{\alpha}_t = \prod_{s=1}^t \alpha_s$, which shows that we can sample any noisy version \mathbf{S}_t within a single step, with a fixed variance β_t . Sampling from $q(\mathbf{S}_t | \mathbf{S}_0, f_\phi(\mathbf{x}))$ is performed via the reparametrization trick. From the above equation, the mean term can be regarded as an interpolation between the initial candidate label \mathbf{S}_0 and the mean of the latent distribution $f_\phi(\mathbf{x})$, gradually changing from the former to the latter throughout the entire forward process. Consequently, \mathbf{S}_t can be computed as:

$$\mathbf{S}_t = \sqrt{\bar{\alpha}_t}\mathbf{S}_0 + (1 - \sqrt{\bar{\alpha}_t})f_\phi(\mathbf{x}) + \sqrt{1 - \bar{\alpha}_t}\epsilon, \quad (4)$$

where $\epsilon \sim \mathcal{N}(\mathbf{0}, \mathbf{I})$. Detailed derivations can be found in Appendix A .

Information Complementarity Label Disambiguation Strategy for Training: When training a diffusion model on a dataset with ambiguous labels, the model learns the conditional score associated with noisy labels. To mitigate this issue, we propose a strategy that leverages complementary information from instances and candidate labels to identify potential ground-truth labels, making the model more resistant to ambiguous labels. Our main assumption is that in the latent space, data points from the same class have the same manifold structure. Therefore, most of the neighbors of the data point should have the same label as the point itself. To this end, we adopt the k -nearest neighbors of the instance embedding features, calculated as a pre-trained encoder f_ϕ , to construct the instance adjacency matrix \mathbf{P} , where $\mathbf{P}_{ij} = 1$ if $f_\phi(\mathbf{x}_i) \in \mathcal{N}_k(f_\phi(\mathbf{x}_j))$ or $f_\phi(\mathbf{x}_j) \in \mathcal{N}_k(f_\phi(\mathbf{x}_i))$, otherwise $\mathbf{P}_{ij} = 0$. The $\mathcal{N}_k(f_\phi(\mathbf{x}_j))$ is defined as the k -nearest neighbor set of $f_\phi(\mathbf{x}_j)$. Furthermore, the candidate labels provide potentially useful information to reduce label ambiguity. For example, if two instances have no overlapping candidate labels, they remain unlinked. Otherwise, a link is established between them. Hence, following Eq.(5), we use the Jaccard distance to measure the similarity between their sets of candidate labels.

$$\mathbf{J}_{ij}(S_i, S_j) = 1 - \frac{|S_i \cup S_j| - |S_i \cap S_j|}{|S_i \cup S_j|} \in [0, 1] \quad (5)$$

where $\mathbf{J} \in \mathbb{R}^{N \times N}$ is label similarity matrix. Therefore, we can perform disambiguation on candidate labels based on the complementary information of \mathbf{P} and \mathbf{J} . For instance, even when two instances are similar ($\mathbf{P}_{ij} > 0$), they won't be linked if they have no shared labels ($\mathbf{J}_{ij} = 0$), because ($\mathbf{P}_{ij} \times \mathbf{J}_{ij} = 0$). Likewise, if they share labels ($\mathbf{J}_{ij} > 0$) but are not similar ($\mathbf{P}_{ij} = 0$), there will still be no connection. Therefore, complementary information between instances and candidate labels can be used to improve the accuracy of disambiguation. The initial pseudo-clean label matrix $\mathbf{S} \in \mathbb{R}^{N \times Q}$ can be calculated by $\mathbf{S} = (\mathbf{P} \odot \mathbf{J})\mathbf{Y}$, where \odot means hadamard product. Then, DDMP is trained to learn the conditional distribution $p(\mathbf{S}|\mathbf{x})$ of disambiguated labels, rather than the label distribution of the data point itself.

Information complementarity label disambiguation strategy enables models to utilize information from multiple potentially more accurate labels to improve their predictive performance. In addition, as the scatter model is effective in modeling multimodal distributions, training the model to mine potential information in the data to generate corresponding labels can reduce the inherent uncertainty in the data annotation process [34]. Therefore, in order to further improve the effectiveness of the model, the pseudo-clean labels in this paper are not fixed but are dynamically updated. This can gradually improve the correspondence between instances and labels, thereby enhancing model performance.

C. The Reverse Process of DDMP

The reverse pass can likewise be modeled as a first-order Markov chain, where the transition dynamics are governed by a learned Gaussian distribution, we start a Q -dimensional Gaussian noise from $\mathbf{S}_T \sim \mathcal{N}(f_\phi(\mathbf{x}), \mathbf{I})$ and reverse the process using $p_\theta(\mathbf{S}_{t-1} | \mathbf{S}_t, \mathbf{x}, f_\phi(\mathbf{x}))$ to reconstruct a label vector \mathbf{S}_0 .

$$p(\mathbf{S}_{0:T}|\mathbf{x}, f_\phi(\mathbf{x})) = p(\mathbf{S}_T) \prod_{t=1}^T p_\theta(\mathbf{S}_{t-1}|\mathbf{S}_t, \mathbf{x}, f_\phi) \quad (6)$$

$$p_\theta(\mathbf{S}_{t-1} | \mathbf{S}_t, \mathbf{x}, f_\phi) = \mathcal{N}\left(\mathbf{S}_{t-1}; \boldsymbol{\mu}_\theta(\mathbf{S}_t, \mathbf{x}, f_\phi, t), \tilde{\beta}_t \mathbf{I}\right) \quad (7)$$

where $\tilde{\beta}_t = \frac{1 - \bar{\alpha}_{t-1}}{1 - \bar{\alpha}_t} \beta_t$, the transition step is Gaussian for an infinitesimal variance β_t . The diffusion model is learned through a neural network to emulate $p_\theta(\mathbf{S}_{t-1} | \mathbf{S}_t, \mathbf{x}, f_\phi(\mathbf{x}))$ by optimizing the evidence lower bound with stochastic gradient descent:

$$\begin{aligned} \mathcal{L} &= \mathbb{E}_q \left[\mathcal{L}_T + \sum_{t>1}^T \mathcal{L}_{t-1} + \mathcal{L}_0 \right], \text{ where} \\ \mathcal{L}_0 &= -\log p_\theta(\mathbf{S}_0 | \mathbf{S}_1, \mathbf{x}, f_\phi) \\ \mathcal{L}_{t-1} &= D_{\text{KL}}(q(\mathbf{S}_{t-1} | \mathbf{S}_t, \mathbf{S}_0, \mathbf{x}, f_\phi) || p_\theta(\mathbf{S}_{t-1} | \mathbf{S}_t, \mathbf{x}, f_\phi)) \\ \mathcal{L}_T &= D_{\text{KL}}(q(\mathbf{S}_T | \mathbf{S}_0, \mathbf{x}, f_\phi) || p(\mathbf{S}_T | \mathbf{x}, f_\phi)) \end{aligned} \quad (8)$$

Eq.(8) focuses on the closeness of $p_\theta(\mathbf{S}_{t-1} | \mathbf{S}_t, \mathbf{x}, f_\phi(\mathbf{x}))$ to the true posterior of the forward process. Following [14], the mean term is written as $\boldsymbol{\mu}_\theta(\mathbf{S}_t, \mathbf{x}, f_\phi, t) = \frac{1}{\alpha_t}(\mathbf{S}_0 - \frac{\beta_t}{\sqrt{1-\alpha_t}}\boldsymbol{\epsilon}_\theta(\mathbf{S}_t, \mathbf{x}, f_\phi, t))$ and the objective can be simplified to $\mathcal{L} = \|\boldsymbol{\epsilon} - \boldsymbol{\epsilon}_\theta(\mathbf{S}_t, \mathbf{x}, f_\phi, t)\|^2$. Then, we predict the ambiguous label $\tilde{\mathbf{S}}_0$, a prediction of \mathbf{S}_0 given \mathbf{S}_t as:

$$\tilde{\mathbf{S}}_0 = \frac{1}{\sqrt{\alpha_t}} [\mathbf{S}_t - (1 - \sqrt{\alpha_t})f_\phi - \sqrt{1 - \alpha_t}\boldsymbol{\epsilon}_\theta(\mathbf{S}_t, \mathbf{x}, f_\phi, t)] \quad (9)$$

Ambiguous Labels: For PLL, each partially labeled instance is independently drawn from a probability distribution, and the key assumption is that correct label y of \mathbf{x} must be in the candidate label set. Therefore, from a generative perspective, it can be expressed as follows:

$$p(S|\mathbf{x}) = \sum_{c=1}^Q p(S|y = y_c)p(y = y_c|\mathbf{x}) \quad (10)$$

The proof of Eq.(10) is provided in Appendix B, which means that the clean class-posterior $p(y = y_c|\mathbf{x})$ can be inferred by utilizing the ambiguous class-posterior $p(S|\mathbf{x})$. Therefore, we introduce a transition-aware matrix $\mathbf{T} = [T_{ij}]^{Q \times Q}$, where $T_{ij} = p(y_i \in S | y = y_j)$, i.e., $p(y|\mathbf{x}) = [\mathbf{T}]^{-1}p(S|\mathbf{x})$. Then, the difficulty is how to estimate the transition-aware matrix.

Estimation of Transition-Aware Matrix: Generally, the transition-aware matrix is non-identifiable without any additional assumption. To implement the DDMP objective, we need to estimate the transition-aware matrix. Concretely, let $\hat{p}(S|\mathbf{x}; \theta)$ parameterized by $\theta \in \mathcal{W}$ be a differentiable model for the ambiguous labels, and $\mathbf{T} \in \mathcal{T}$ be an estimator for the transition-aware matrix. Assuming that the function of $\hat{p}(S|\mathbf{x}; \theta)$ is sufficiently large enough, this means that there exists an optimal parameter $\theta^* \in \mathcal{W}$ that makes $[\mathbf{T}]^{-1}\hat{p}(S|\mathbf{x}; \theta^*)$ and $p(y|\mathbf{x})$ equal everywhere. In practice, we use an expressive deep neural network, the reverse model of DDMP, to approximate $p(S|\mathbf{x})$. Therefore, the transition-aware matrix is estimated by:

$$\mathbf{T}_{ij}^e = \frac{\sum_{k=1}^N \mathbb{I}(y_j \in S_k) \mathbf{S}_{ki}^e}{\sum_{k=1}^N \mathbf{S}_{ki}^e} \quad (11)$$

where $\mathbb{I}(\cdot)$ is an indicator function. e is the number of iterations. Since \mathbf{S} is updated asymptotically, \mathbf{T} is also dynamically estimated based on \mathbf{S} to approximate the true value. We propose a softened and moving-average style strategy to update the ambiguous labels. The pseudo-clean labels are updated by:

$$\mathbf{S}^{e+1} = \text{Normalize}((\mathbf{S}^e + [\mathbf{T}^e]^{-1}\tilde{\mathbf{S}}_0^e)\mathbf{S}^e) \quad (12)$$

where $\text{Normalize}(\cdot)$ is normalization function. When $e = 1$, $\mathbf{S}^1 = \mathbf{S}$ is initial pseudo-clean label matrix. Due to the fact that the parameters of the model are still far from optimal during early training, a moving-average strategy is applied to gradually adjust the pseudo-clean labels toward their true values while maintaining stable training dynamics. As illustrated in Figure 2, with the progression of iterative training, the

Algorithm 1 DDMP Framework

Input: Training set \mathcal{D} , label confidence matrix \mathbf{Y} , pre-trained encoder f_ϕ .

Initialization

Calculate initial pseudo-clean matrix \mathbf{S} according to \mathbf{P} and \mathbf{J} ;

while not converged **do**

Sample time slice $t \sim \{1, \dots, T\}$, data (\mathbf{x}, \mathbf{S}) , and noise $\boldsymbol{\epsilon} \sim \mathcal{N}(\mathbf{0}, \mathbf{I})$

Sample \mathbf{S}_t , and convert it to a one-hot vector \mathbf{S}_0

Optimize the loss with a gradient descent step

$\mathcal{L} = \|\boldsymbol{\epsilon} - \boldsymbol{\epsilon}_\theta(\mathbf{S}_t, \mathbf{x}, f_\phi, t)\|^2$

Update transition-aware matrix \mathbf{T} according to Eq.(11)

Update pseudo-clean label matrix \mathbf{S} according to

Eq.(12)

end while

ground-truth label is progressively identified through Eq.(12), and the refined labels can improve the information matching between the instances and labels. Therefore, the forward denoising and backward reverse disambiguation processes are alternately and iteratively improved in their performance. The training process is considered complete once both components achieve satisfactory performance. We further rigorously draw a resemblance of DDMP with a classical EM-style algorithm in Section IV-I. Algorithm 1 summarizes the complete procedure of DDMP.

IV. EXPERIMENTS

The experimental results presented in this section demonstrate the superior performance of the proposed method on partial label datasets when compared to existing PLL techniques. Code and data can be found at: <https://github.com/fanjinfulcool/DDMP>.

A. Datasets

(1) Real-World PLL datasets.

To comprehensively and effectively evaluate the performance of the proposed DDMP method, we employ five widely used real-world partial label datasets, including Lost [2], BirdSong [36], Soccer Player [37], MSRCv2 [15], and Yahoo! News [38]. The details of these datasets, including *number of features* (#FES), *number of instances* (#INS), *the mean number of ambiguous labels* (#EAL), and *number of labels* (#LAS), are summarized in Table I. These datasets encompass diverse application scenarios, including *Object Classification*, *Automatic Face Naming* and *Bird Song Classification*.

(2) Synthesized PLL datasets.

To assess the effectiveness of the proposed algorithm, we utilize five commonly used benchmark datasets, including MNIST [39], Kuzushiji-MNIST [40], CIFAR-10 [41], Fashion-MNIST [42], and CIFAR-100 [41]. The partial label datasets are constructed following the standard synthesis procedure in PLL [10], where candidate label sets for each instance are formed through $Q - 1$ independent selections of noise labels. The parameter q controls the probability

TABLE I
COMPREHENSIVE INFORMATION ON REAL-WORLD DATASETS

Data	FEA	INS	MAL	LAS	Scenarios
MSRCv2	48	1758	3.16	23	<i>Object Classification</i>
Lost	108	1122	2.33	16	<i>Automatic Face Naming</i>
BirdSong	38	4998	2.18	13	<i>Bird Song Classification</i>
Yahoo! News	163	22991	1.91	219	<i>Automatic Face Naming</i>
SoccerPlayer	279	17472	2.09	171	<i>Automatic Face Naming</i>

of each noise label being included. Notably, higher values of q increase the likelihood of instances having more noise labels, thereby raising the difficulty of label disambiguation. We experiment with q values from the set $\{0.1, 0.3, 0.5\}$ for MNIST, KuzushijiMNIST, Fashion-MNIST, CIFAR-10 and $\{0.01, 0.05, 0.1\}$ for CIFAR-100.

B. Compared Methods

To demonstrate the superiority of the proposed DDMP algorithm, we conducted comparisons with state-of-the-art PLL methods, including deep learning based on PLL methods PRODEN [10], LW [21], CAVL [43], CRDPLL [44] and PiCO [24], and the deep learning based on instance-dependent PLL methods VALEN [27], ABLE [28], and DIRK [29]. Parameter configurations for compared methods replicate literature specifications.

- VALEN [27]: Predictive models are trained iteratively at each period using candidate labels and label distributions. [suggested configuration: Weight decay (10^{-4}), training batch(500), learning rate (10^{-2})].
- PRODEN [10]: Model updating and label disambiguation are done step-by-step using an incremental recognition approach. [suggested configuration: Weight decay (10^{-5}), training batch(500), learning rate (10^{-3})].
- LW [21]: The trade-off between candidate label loss and non-candidate label loss is considered using leverage weighted loss. [suggested configuration: Weight decay (10^{-5}), training batch(500), learning rate (10^{-3})].
- CAVL [43]: Truth labels are identified using class activation graphs and their promotion form class activation values to improve partial label learning, and ultimately real labels are progressively identified through the intrinsic representation of the model. [suggested configuration: Learning rate (10^{-3}), training batch(250), weight decay (10^{-3})].
- PICO [24]: Utilizing the idea of learning by contrast for representation learning and ultimately disambiguation through prototype updating. [suggested configuration: Learning rate (10^{-2}), training batch(500), weight decay (10^{-3})].
- ABLE [28]: Boosting PLL performance via contrastive learning explicitly leveraging label ambiguity. [suggested configuration: Learning rate (10^{-2}), training batch(500), weight decay (10^{-3})].
- DIRK [29]: A partial label learning algorithm synergizing knowledge distillation and contrastive learning to improve

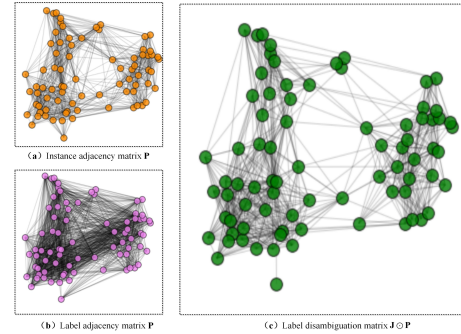


Fig. 3. The visualization of adjacency matrix graph.

model robustness. [suggested configuration: Learning rate (10^{-2}), training batch(500), weight decay (10^{-3})].

- CRDPLL [44]: A PLL algorithm that enhances model performance through the use of consistency regularization. [suggested configuration: Training batch(64), learning rate (10^{-1}), weight decay (10^{-4}), $T' = 100$, $\lambda = 1$, and $K = 3$].

C. Implementation Details

As shown in Figure 2, the DDMP consists of a pre-trained instance encoder f_ϕ , an instance encoder layer, an instance-guided cross attention, a label-guided cross attention, and a series of feed-forward layers. Two cross attention mechanisms are used to mine potential effective information of two encoding features through information guidance. These features are then combined with a Hadamard product and time embedding. A sequence of feed-forward networks predicts the noise term ϵ_θ , utilizing batch normalization layers and Softplus activation functions. Our implementation was executed using PyTorch, and all experiments were conducted with NVIDIA GeForce RTX 4090 GPU. The DDMP framework is trained for 200 epochs with Adam optimization and 256 batch size. For the nearest neighbors, we set $k = 10$. Following [34], the sampling trajectory is 10 and $T = 1000$. In our experiments, we use SimCLR [45] and CLIP [46] as pre-trained models respectively as shown in [34]. For SimCLR, we use MLP for MNIST, KuzushijiMNIST, and Fashion-MNIST, and ResNet34 for CIFAR100 and CIFAR10 as the pre-trained encoder. Since the real-world partially labeled datasets are processed, we directly use these data as encoding features. For CLIP, we utilized the Vision Transformer encoder (ViT-L/14), pre-trained within the CLIP framework, as it represents the top-performing architecture for this task.

D. Main Experiment Results

1) Real-world Partially Labeled Datasets:

The proposed algorithm is evaluated on real-world partially labeled datasets through ten-fold cross-validation to assess its effectiveness. Specifically, Table II presents the test results of DDMP compared to other algorithms across five real-world datasets.

- Across 40 experiments (5 real-world datasets \times 8 comparison algorithms), DDMP significantly outperforms all other methods in 85.0% of the cases.

TABLE II
ACCURACY COMPARISONS ON REAL-WORLD PARTIALLY LABELED DATASETS.

Method	Datasets				
	Lost	MSRCv2	Birdsong	SoccerPlayer	YahooNews
PiCO	65.33 \pm 0.75%	49.14 \pm 0.57%	61.29 \pm 2.10%	55.13 \pm 1.48%	68.71 \pm 0.22%
CAVL	63.11 \pm 0.72%	52.84 \pm 1.16%	70.50 \pm 0.92%	54.27 \pm 0.37%	63.86 \pm 0.58%
VALEN	71.56 \pm 0.80%	45.89 \pm 0.55%	72.30 \pm 0.49%	53.91 \pm 0.12%	67.73 \pm 0.32%
PRODEN	65.17 \pm 0.72%	52.00 \pm 0.46%	63.38 \pm 0.52%	51.45 \pm 0.19%	59.06 \pm 0.38%
LW	67.11 \pm 1.78%	47.15 \pm 0.75%	66.50 \pm 0.73%	49.15 \pm 0.38%	47.03 \pm 0.37%
ABLE	68.93 \pm 1.11%	53.66 \pm 0.95%	74.70 \pm 0.78%	62.77 \pm 0.42%	53.35 \pm 0.35%
DIRK	74.26 \pm 0.58	44.61 \pm 0.32%	71.28 \pm 0.21%	53.37 \pm 0.48%	61.38 \pm 0.22
CRDPLL	64.55 \pm 0.31%	49.14 \pm 0.87%	72.00 \pm 0.62%	54.47 \pm 0.22%	65.23 \pm 0.74%
DDMP	74.58 \pm 0.21%	53.71 \pm 0.28%	80.36 \pm 0.23%	62.83 \pm 0.24%	54.56 \pm 0.37%

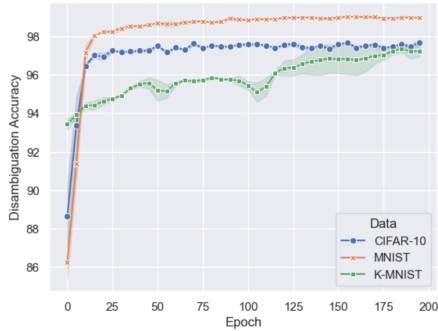


Fig. 4. Convergence results of DDMP on benchmark datasets.

- As shown in Table II, DDMP achieves superior performance on real-world datasets compared to other deep learning-based PLL methods. Specifically, on the Lost, MSRCv2, and Birdsong datasets, DDMP outperforms the best competing method in disambiguation accuracy by 0.32%, 0.05%, 5.66%, respectively. This advantage stems from the ability of DDMP to utilize potential information within instances and candidate labels, thereby reducing the effect of ambiguous labels and mitigating the influence of misleading nearest neighbor instances when generating pseudo-clean labels. Additionally, DDMP effectively learns to eliminate the impact of ambiguous labels during the reverse generative process.

2) Synthesized Partially Labeled Datasets:

The comparison algorithms are evaluated on various synthesized benchmark datasets to thoroughly validate the effectiveness of DDMP. Despite comparison algorithms exhibiting specialized strengths per dataset in Table III, DDMP achieves universal performance dominance, outperforming all comparative methods in most cases.

- As illustrated in Table III, DDMP consistently achieves better disambiguation results across datasets with different degrees of label ambiguity. Specifically, out of 120 experiments (8 comparison algorithms \times 15 synthesized benchmark datasets), DDMP(CLIP) significantly outperforms the comparative methods in 97.5% cases. Meanwhile, DDMP(SimCLR) is 70.8% higher than comparative methods and achieves comparable performance to PiCO.
- Across all evaluated synthesized benchmark datasets, DDMP(CLIP) demonstrates consistently superior perfor-

mance relative to other deep learning PLL methods. Notably, on the CIFAR-10 and CIFAR-100 datasets, it outperforms the best compared PLL algorithm by 3.51% and 32.2% respectively.

- When compared with deep learning-based PLL methods, DDMP(SimCLR) consistently performs better than VALEN, PRODEN, and LW in most instances. Specifically, on the Kuzushiji-MNIST, CIFAR-10 and CIFAR-100 datasets, DDMP(SimCLR) outperforms the best deep learning PLL method by 3.56%, 9.65%, 2.32%.
- It is important to highlight that DDMP achieves high performance on synthetic benchmarks and remains robust even as the value of q grows, further validating its effectiveness in addressing the PLL problem. Moreover, for the CLIP pre-training model, this paper only used the instance encoder, and did not use the label encoder. For DDMP, by comparing the two pre-training models of SimCLR and CLIP, it can be found that good encoding features can significantly improve the disambiguation performance of ambiguous labels in PLL. This insight offers a promising direction for future research, suggesting that the strengths of unsupervised contrastive learning can be harnessed to mitigate the impact of ambiguous labels.

To better verify the disambiguation effectiveness of DDMP, we tested the performance of different PLL methods on a large number of datasets. Despite the growing label ambiguity with increasing q , DDMP consistently delivers superior disambiguation performance, surpassing nearly all other compared PLL methods. This impressive result can be attributed to the integration of the information complementarity label disambiguation strategy and the estimation of the transition-aware matrix, which together effectively extract valuable information from instances and candidate labels, enabling continuous refinement of the label matrix and mitigating the influence of ambiguity. Specifically, DDMP reformulates the label disambiguation problem from the perspective of generative models, where labels are generated by iteratively refining initial random guesses. This perspective enables the diffusion model to learn how label information is generated stochastically, effectively mitigating the impact of ambiguous labeling. It is also noteworthy that pre-trained instance encoders remain unaffected by label ambiguity, as they are trained via self-supervised learning and significantly enhance the adversarial robustness of the model [47] [34].

TABLE III
COMPARATIVE DISAMBIGUATION ACCURACY (MEAN \pm STD) ACROSS DATASETS.

Method	q	Datasets				
		MNIST	Fashion-MNIST	Kuzushiji-MNIST	CIFAR-10	CIFAR-100
PiCO	0.1	98.97 \pm 0.12%	93.36 \pm 0.09%	97.68 \pm 0.06%	94.54 \pm 0.05%	71.02 \pm 0.29%
	0.3	98.85 \pm 0.14%	93.12 \pm 0.12%	97.34 \pm 0.03%	94.13 \pm 0.08%	70.29 \pm 0.29%
	0.5	98.63 \pm 0.03%	92.88 \pm 0.03%	97.15 \pm 0.12%	93.85 \pm 0.15%	58.16 \pm 0.34%
CAVL	0.1	98.95 \pm 0.04%	90.32 \pm 0.08%	93.73 \pm 0.16%	83.37 \pm 0.07%	45.80 \pm 0.13%
	0.3	98.90 \pm 0.15%	89.77 \pm 0.04%	93.57 \pm 0.11%	81.45 \pm 0.22%	39.87 \pm 0.33%
	0.5	98.71 \pm 0.04%	88.92 \pm 0.11%	91.57 \pm 0.22%	73.25 \pm 0.17%	21.55 \pm 0.12%
VALEN	0.1	98.75 \pm 0.02%	90.72 \pm 0.06%	92.67 \pm 0.06%	83.21 \pm 0.10%	66.79 \pm 0.13%
	0.3	98.66 \pm 0.03%	90.16 \pm 0.06%	91.75 \pm 0.22%	82.87 \pm 0.26%	66.15 \pm 0.25%
	0.5	98.32 \pm 0.02%	89.51 \pm 0.04%	90.40 \pm 0.03%	81.88 \pm 0.20%	65.21 \pm 0.33%
PRODEN	0.1	98.91 \pm 0.03%	88.27 \pm 0.03%	91.11 \pm 0.03%	80.45 \pm 0.24%	50.42 \pm 0.28%
	0.3	98.71 \pm 0.02%	87.83 \pm 0.04%	90.67 \pm 0.04%	79.05 \pm 0.11%	50.29 \pm 0.29%
	0.5	98.57 \pm 0.03%	87.01 \pm 0.03%	89.00 \pm 0.05%	77.52 \pm 0.18%	46.81 \pm 0.32%
LW	0.1	98.76 \pm 0.03%	88.18 \pm 0.05%	92.78 \pm 0.04%	81.43 \pm 0.13%	51.63 \pm 0.10%
	0.3	98.64 \pm 0.02%	88.02 \pm 0.04%	91.28 \pm 0.03%	80.95 \pm 0.17%	46.54 \pm 0.17%
	0.5	98.41 \pm 0.03%	87.66 \pm 0.06%	86.55 \pm 0.06%	78.72 \pm 0.17%	34.56 \pm 0.45%
ABLE	0.1	96.72 \pm 0.13%	92.04 \pm 0.14%	94.89 \pm 0.03%	92.98 \pm 0.31%	52.81 \pm 0.12%
	0.3	96.5 \pm 0.52%	91.91 \pm 0.09%	94.35 \pm 0.28%	92.37 \pm 0.15%	46.26 \pm 0.45%
	0.5	96.41 \pm 0.06%	91.33 \pm 0.17%	92.98 \pm 0.31%	91.67 \pm 0.22%	45.13 \pm 0.21%
DIRK	0.1	98.92 \pm 0.25%	93.71 \pm 0.10%	97.13 \pm 0.32%	92.41 \pm 0.23%	67.71 \pm 0.51%
	0.3	98.54 \pm 0.29%	92.1 \pm 0.19%	96.49 \pm 0.47%	92.14 \pm 0.12%	64.47 \pm 0.32%
	0.5	98.31 \pm 0.13%	91.23 \pm 0.24%	96.13 \pm 0.51%	91.34 \pm 0.14%	64.28 \pm 0.47%
CRDPLL	0.1	98.72 \pm 0.22%	93.21 \pm 0.24%	97.13 \pm 0.57%	94.71 \pm 0.18%	75.31 \pm 0.61%
	0.3	98.64 \pm 0.19%	92.53 \pm 0.31%	96.55 \pm 0.45%	94.27 \pm 0.24%	76.67 \pm 0.18%
	0.5	98.32 \pm 0.33%	91.47 \pm 0.20%	96.21 \pm 0.61%	93.84 \pm 0.11%	71.21 \pm 0.34%
DDMP(SimCLR)	0.1	98.88 \pm 0.21%	91.03 \pm 0.32%	97.29 \pm 0.13%	93.02 \pm 0.32%	69.11 \pm 0.43%
	0.3	98.76 \pm 0.13%	90.84 \pm 0.14%	96.86 \pm 0.08%	92.57 \pm 0.41%	68.13 \pm 0.23%
	0.5	98.53 \pm 0.09%	90.36 \pm 0.41%	96.35 \pm 0.21%	91.89 \pm 0.27%	66.29 \pm 0.52%
DDMP(CLIP)	0.1	99.16 \pm 0.03%	93.51 \pm 0.34%	94.01 \pm 0.17%	97.79 \pm 0.12%	84.03 \pm 0.05%
	0.3	99.06 \pm 0.12%	93.24 \pm 0.28%	93.89 \pm 0.24%	97.71 \pm 0.17%	83.37 \pm 0.16%
	0.5	98.90 \pm 0.23%	92.97 \pm 0.56%	93.45 \pm 0.31%	97.36 \pm 0.23%	81.65 \pm 0.09%

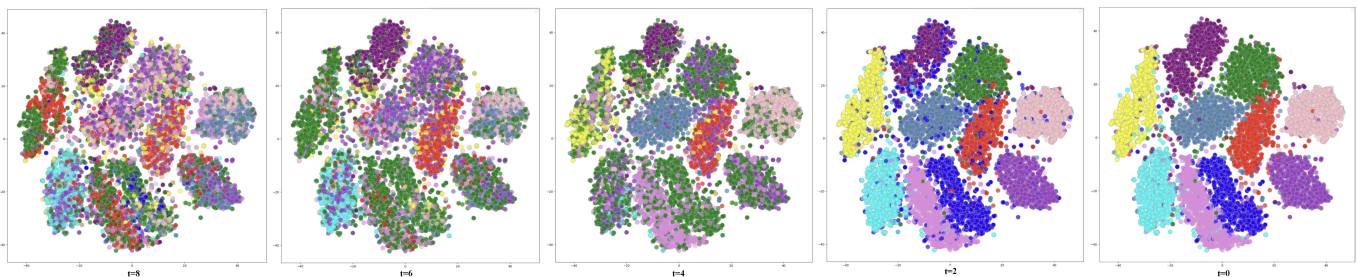


Fig. 5. T-SNE visualization of MNIST dataset during DDMP reverse generation process.

E. Ablation Study

To better assess the role of each component within the DDMP method, ablation experiments were performed on two specific parts, i.e., the information complementarity label disambiguation strategy and the estimation of the transition-aware matrix are also conducted. From the ablation results presented in Table IV, the following conclusions can be derived.

- Compared with DDMP-w/o-I, DDMP shows a good disambiguation ability. This is attributed to the complementary information between instances and candidate labels, which helps mitigate the influence of ambiguous labels and effectively guides learning process of the model. To better illustrate this point, the adjacency matrices are visualized. From Figure 3, it can be seen that the connection lines in points \mathbf{P} and \mathbf{J} are significantly

reduced, as the potential information of candidate labels can effectively reduce the impact of negative nearest neighbor instance in the disambiguation process, thereby learning accurate pseudo-clean labels.

- DDMP achieves better disambiguation results compared to DDMP-w/o-T, as the label transition-aware matrix helps mitigate the effects of ambiguous labels by capturing the underlying distribution of the true labels.
- The variant DDMP-w/o-IT suffers a slight drop in performance. This is attributed to the mutual reinforcement between the initial label disambiguation and the transition-aware matrix, which together enhance the ability of the model to resolve label ambiguity. As training advances, the model progressively uncovers the true labels, and these increasingly accurate labels further steer the learning process, leading to improved disambiguation

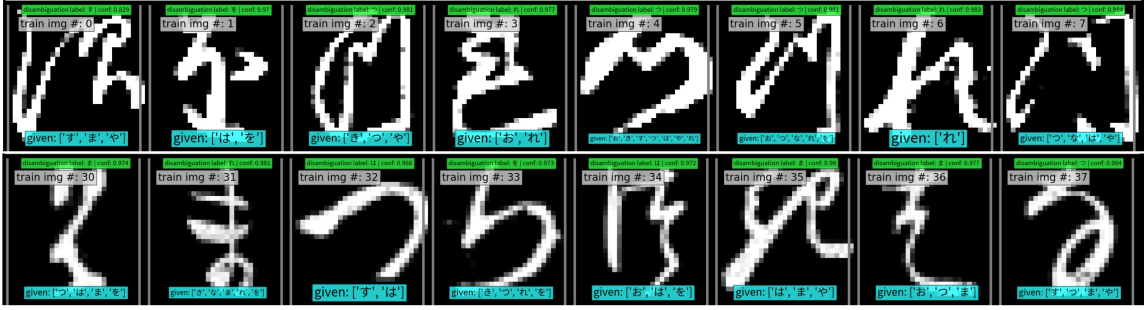
(a) CIFAR-10 dataset, $q = 0.3$ (b) Kuzushiji-MNIST dataset, $q = 0.3$

Fig. 6. Visual Representation of Disambiguation Results from the DDMP Algorithm.

TABLE IV
ABLATION STUDY OF DDMP(SIMCLR) ON CIFAR-10 ($q = 0.3$) AND
BIRDSONG DATASETS.

Ablation	I	T	CIFAR-10	Birdsong
DDMP	✓	✓	92.57 ± 0.41%	80.36 ± 0.23%
DDMP-w/o-I	✗	✓	88.34 ± 0.07%	78.16 ± 0.34%
DDMP-w/o-T	✓	✗	88.79 ± 0.34%	77.24 ± 0.41%
DDMP-w/o-IT	✗	✗	78.77 ± 0.32%	71.52 ± 0.27%

performance.

F. Convergence Analysis

To more intuitively demonstrate the convergence of DDMP, we analyze its performance on three synthetic benchmark datasets, specifically using datasets with $q = 0.3$. As shown in Figure 4, DDMP achieves effective label disambiguation on these benchmarks. As training proceeds, the model steadily approaches a stable performance level, which empirically verifies its convergence. Additionally, the results on both synthetic and real-world datasets indicate that DDMP not only excels in disambiguation but also maintains strong stability throughout the training process.

G. Visualization Analysis

To more intuitively reflect the superiority of DDMP, Figure 5 demonstrates the visualization of the reverse denoising and disambiguation process of DDMP, which transforms the latent distribution into the ground-truth distribution of labels through a series of multi-step inverse operations. As shown in Figure 5, each cluster achieved accurate classification, which

also verifies the effectiveness of the DDMP algorithm in label denoising and disambiguation. To further highlight the advantages of the DDMP algorithm, disambiguation visualization is conducted on the CIFAR10 and Kuzushiji-MNIST datasets with a noise level of $q = 0.3$. As illustrated in Figure 6, the blue boxes indicate the candidate label sets for each instance, while the green boxes represent the disambiguation results along with the confidence scores for the corresponding label classes. Therefore, it is evident that the DDMP can effectively achieve accurate disambiguation even in the presence of a significant number of ambiguous labels.

H. Uncertainty Quantification of PLL Methods

When deploying machine learning systems, it is essential that algorithms are not only accurate but also reliable and capable of recognizing potential errors, as this better reflects the effectiveness and reliability of the model [48] [29]. Therefore, we conducted a preliminary analysis of the output uncertainty associated with various PLL methods, as illustrated in Figure 7. The results indicate that DDMP enables the diffusion model to learn how label information is randomly generated by mining potential valid information between instances. This not only effectively reduces the impact of label ambiguity, but also makes the model more robust and reliable, thereby improving the credibility of the model output and achieving competitive *expected calibration error* (ECE) scores. Specifically, our method achieves the lowest ECE score among the comparison methods on CIFAR10. The analysis reveals a near-perfect alignment between actual accuracy and average consistency, both of which closely follow the ideal calibration line. The extremely low expected calibration error (ECE=0.007) demonstrates excellent calibration performance.

Especially within the high consistency range (0.6-1.0), the deviation between consistency and accuracy can be ignored, indicating an extremely accurate reliability assessment of high certainty predictions. Although the sample size is small in the low consistency range (0.0-0.4), the calibration quality is still strong with only slight statistical fluctuations. A significant feature appears in the data distribution, the actual accuracy strictly monotonically improves over the consistency interval, and the deviation of the accuracy from the predicted consistency in each interval is minimal. This strong positive correlation indicates superior probabilistic calibration. Most notably, in the high confidence interval of (0.8-1.0), the actual accuracy is close to the theoretical maximum, which provides convincing evidence for the reliability of the model in high-certainty predictions.

I. Convergence proof of DDMP

In this section, we provide a theoretical explanation of why DDMP helps disambiguate candidate labels. This paper intends to interpret the DDMP algorithm as an *expectation-maximization*(EM) algorithm. The EM algorithm can be used to deduce how to model and update the ambiguous labels through the transition-aware matrix, thereby improving the classification performance of the model. According to Eq.(9) and Eq.(10), we can further simplify the \mathcal{L}_0 loss in Eq.(9) as,

$$\mathcal{L}_0 = -\log p(\mathbf{S}_0 | \mathbf{S}_1, \mathbf{x}, \mathbf{T}, f_\phi, \theta) \quad (13)$$

Introducing the unobserved ground-truth label vector \mathbf{y} , the log likelihood of the complete data is,

$$\mathcal{L}_0 = -\log p(\mathbf{S}_0, \mathbf{y} | \mathbf{S}_1, \mathbf{x}, \mathbf{T}, f_\phi, \theta) = -\log p(\mathbf{S}_0, \mathbf{y} | \mathbf{x}, \mathbf{T}, \theta) \quad (14)$$

Using joint probability decomposition, we can get,

$$p(\mathbf{S}_0, \mathbf{y} | \mathbf{x}, \mathbf{T}, \theta) = p(\mathbf{S}_0 | \mathbf{y}, \mathbf{T}) p(\mathbf{y} | \mathbf{x}, \theta) \quad (15)$$

Therefore, the Eq.(14) can be written as,

$$\mathcal{L}_0 = -\log p(\mathbf{S}_0 | \mathbf{y}, \mathbf{T}) - \log p(\mathbf{y} | \mathbf{x}, \theta) \quad (16)$$

Then, we show that the DDMP implicitly maximizes the likelihood as follows,

E-Step: In the E-step, we compute the posterior probability $p(\mathbf{y} | \mathbf{S}_0, \mathbf{x}, \mathbf{T}, \theta)$ as the distribution of the unobserved ground-truth label \mathbf{y} .

$$p(\mathbf{y} = y_c | \mathbf{S}_0, \mathbf{x}, \mathbf{T}, \theta) = \frac{p(\mathbf{S}_0 | \mathbf{y} = y_c, \mathbf{T}) P(\mathbf{y} = y_c | \mathbf{x}, \theta)}{\sum_{i=1} p(\mathbf{S}_0 | \mathbf{y} = y_i, \mathbf{T}) P(\mathbf{y} = y_i | \mathbf{x}, \theta)} \quad (17)$$

where Eq.(17) is the posterior probability that the ground-truth label is y_c . Therefore, according to Eq.(12), the candidate labels can be smoothly disambiguated to calculate a more stable posterior probability \mathbf{S} .

M-Step: In the M-step, the model parameters θ and the transition-aware matrix \mathbf{T} are updated to maximize the expected log-likelihood calculated in the E step. When \mathbf{T} is fixed and the model parameters θ are updated,

$$\mathcal{L}_\theta = -\mathbf{S} \log p(\mathbf{y} | \mathbf{x}, \theta) \quad (18)$$

This is equivalent to weighted maximum likelihood estimation. When model parameters θ is fixed and the transition-aware matrix \mathbf{T} are updated,

$$\mathcal{L}_\mathbf{T} = -\mathbf{S} \log p(\mathbf{S}_0 | \mathbf{y}, \mathbf{T}) \quad (19)$$

By using the Lagrange multiplier method, constraining $\mathbf{T}_{ij} > 0$ and $\sum_{j=1}^Q \mathbf{T}_{ij} = 1$, the final update formula is:

$$\mathbf{T}_{ij}^e = \frac{\sum_{i=1}^N \mathbb{I}(y_j \in S_i) \mathbf{S}_{ij}}{\sum_{i=1}^N \mathbf{S}_{ij}} \quad (20)$$

where $\mathbb{I}(\cdot)$ is an indicator function. The essence of the M-step is to minimize the classification loss. Therefore, during the entire training process of DDMP, the E-step estimates the possibility (i.e., posterior distribution) that each instance belongs to a potential ground-truth label, which provides a weighted basis for parameter optimization in the M-step. In the M-step, the update of the transition-aware matrix \mathbf{T} is adjusted by the weighted distribution of the instances to ensure that each item of \mathbf{T} satisfies the constraints at the same time. The transition-aware matrix \mathbf{T} is used to characterize how the ground-truth label is perturbed by ambiguous labels, thereby generating disambiguation labels. When these two components perform well, the entire training process converges. By iteratively updating \mathbf{T} , gradually approaching the most realistic label distribution.

V. CONCLUSION

In this paper, an iterative diffusion disambiguation model, called DDMP, for learning on the partial label dataset is proposed. The highlight of DDMP is that it reformulates the label disambiguation problem from the perspective of generative models, where labels are disambiguated through the reverse denoising process. Specifically, an information complementarity label disambiguation strategy is proposed, which can explore the potential information of instances and candidate labels to reduce the impact of ambiguous labels and negative nearest neighbor instances to construct pseudo-clean labels and be used for downstream disambiguation learning. Furthermore, a transition-aware matrix is introduced to estimate the potential ground-truth labels, which are dynamically updated during the diffusion generation. Meanwhile, theoretical analysis shows that this matrix update can be interpreted from an EM-style algorithm perspective. During training, the ground-truth label is progressively refined, improving the classifier. We evaluate the DDMP on partial label datasets and obtain state-of-the-art performance.

APPENDIX

A. Forward process derivation of DDMP

The forward diffusion process, where the latent variable has a non-zero mean distribution $\mathbf{S}_T \sim \mathcal{N}(f_\phi(\mathbf{x}), \mathbf{I})$, can be expressed in a closed-form representation,

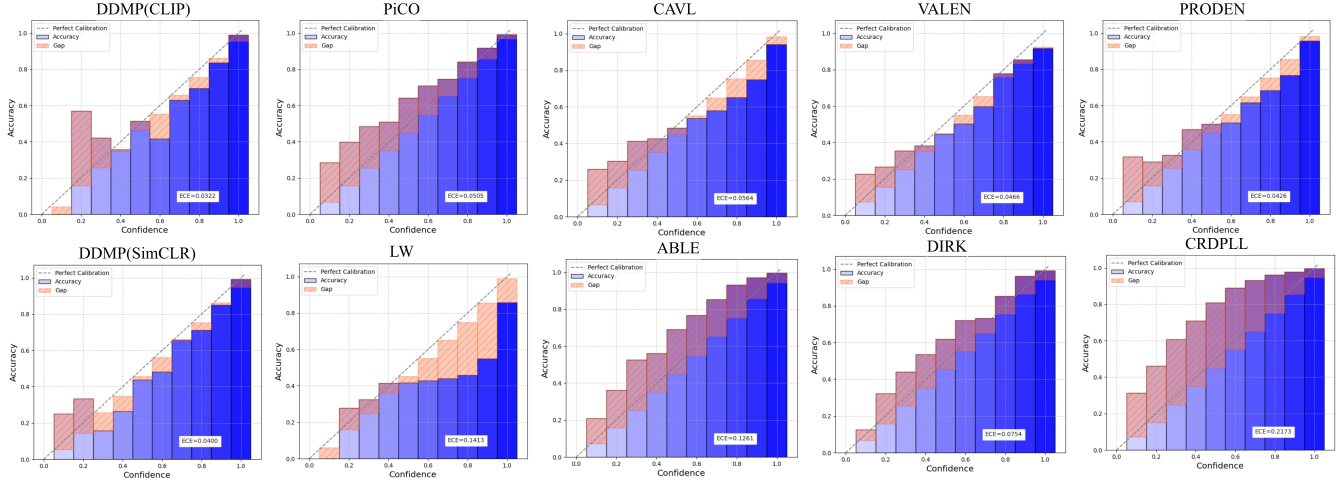


Fig. 7. Reliability diagram and expected calibration error.

$$q(\mathbf{S}_t | \mathbf{S}_{t-1}, f_\phi(\mathbf{x})) = \mathcal{N}(\mathbf{S}_t; \sqrt{1 - \beta_t} \mathbf{S}_{t-1} + (1 - \sqrt{1 - \beta_t}) f_\phi(\mathbf{x}), \beta_t \mathbf{I}) \quad (21)$$

where $f_\phi(\mathbf{x})$ is a mean estimator set by the encoder. Let $\alpha_t = 1 - \beta_t$, then we have,

$$\mathbf{S}_{t-1} = \sqrt{\alpha_{t-1}} \mathbf{S}_{t-2} + (1 - \sqrt{\alpha_{t-1}}) f_\phi(\mathbf{x}) + (\sqrt{1 - \alpha_{t-1}}) \epsilon_{t-1} \quad (22)$$

$$\mathbf{S}_t = \sqrt{\alpha_t} \mathbf{S}_{t-1} + (1 - \sqrt{\alpha_t}) f_\phi(\mathbf{x}) + (\sqrt{1 - \alpha_t}) \epsilon_t \quad (23)$$

By substituting \mathbf{S}_{t-1} into Eq.(23), we can obtain,

$$\begin{aligned} \mathbf{S}_t &= \sqrt{\alpha_t} \left(\sqrt{\alpha_{t-1}} \mathbf{S}_{t-2} + \sqrt{1 - \alpha_{t-1}} \epsilon_{t-1} + (1 - \sqrt{\alpha_{t-1}}) f_\phi(\mathbf{x}) \right) \\ &\quad + \sqrt{1 - \alpha_t} \epsilon_t + (1 - \sqrt{\alpha_t}) f_\phi(\mathbf{x}) \\ &= \sqrt{\alpha_t \alpha_{t-1}} \mathbf{S}_{t-2} + \sqrt{\alpha_t} \sqrt{1 - \alpha_{t-1}} \epsilon_{t-1} + \sqrt{1 - \alpha_t} \epsilon_t \\ &\quad + \sqrt{\alpha_t} (1 - \sqrt{\alpha_{t-1}}) f_\phi(\mathbf{x}) + (1 - \sqrt{\alpha_t}) f_\phi(\mathbf{x}) \end{aligned} \quad (24)$$

It is known that ϵ_{t-1} and ϵ_t conform to $\mathcal{N}(\mathbf{0}, \mathbf{I})$ Gaussian distribution, so according to the Gaussian function superposition formula, the above formula can be simplified to,

$$\mathbf{S}_t = \sqrt{\alpha_t \alpha_{t-1}} \mathbf{S}_{t-2} + (1 - \sqrt{\alpha_t \alpha_{t-1}}) f_\phi(\mathbf{x}) + \sqrt{1 - \alpha_t \alpha_{t-1}} \epsilon \quad (25)$$

By mathematical induction, we can obtain the relationship between \mathbf{S}_t and \mathbf{S}_0 ,

$$\begin{aligned} \mathbf{S}_t &= \sqrt{\alpha_t \alpha_{t-1} \cdots \alpha_0} \mathbf{S}_0 + (1 - \sqrt{\alpha_t \alpha_{t-1} \cdots \alpha_0}) f_\phi(\mathbf{x}) \\ &\quad + \sqrt{1 - \alpha_t \alpha_{t-1} \cdots \alpha_0} \epsilon \end{aligned} \quad (26)$$

Let $\bar{\alpha}_t = \alpha_t \alpha_{t-1} \cdots \alpha_0 = \prod_t \alpha_t$, we have

$$\mathbf{S}_t = \sqrt{\bar{\alpha}_t} \mathbf{S}_0 + (1 - \sqrt{\bar{\alpha}_t}) f_\phi(\mathbf{x}) + \sqrt{1 - \bar{\alpha}_t} \epsilon \quad (27)$$

B. Proof of the PLL generative perspective

From a generative perspective, the PLL can be expressed as follows:

$$p(S|\mathbf{x}) = \sum_{c=1}^Q p(S|y = y_c) p(y = y_c | \mathbf{x}) \quad (28)$$

We provide a detailed derivation for the Eq.(28). According to the Bayes' theorem, the conditional probability $p(S|\mathbf{x})$ can be expressed as:

$$p(S|\mathbf{x}) = \frac{p(S, \mathbf{x})}{p(\mathbf{x})} = \frac{\sum_{c=1}^Q p(S|y = y_c) p(\mathbf{x}, y = y_c)}{p(\mathbf{x})} \quad (29)$$

Here, $p(\mathbf{x}, y = y_c)$ represents the joint probability distribution of instance \mathbf{x} and correct label $y = y_c$. Eq.(29) assumes that $p(S|\mathbf{x}, y) = p(S|y)$, given the correct label y , the candidate label set S is independent of the instance \mathbf{x} . According to the definition of PLL, if $y_c \notin S$, we have $p(S|y = y_c) = 0$. Therefore, we can further simplify this expression.

$$\begin{aligned} p(S|\mathbf{x}) &= \sum_{c=1}^Q p(S|y = y_c) p(y = y_c | \mathbf{x}) \\ &= \sum_{y_c \in S} p(S|y = y_c) p(y = y_c | \mathbf{x}) \end{aligned} \quad (30)$$

ACKNOWLEDGMENT

This work was funded by the Natural Science Foundation of Shandong Province (Project No. ZR2024QF119), the National Natural Science Foundation of China (Project No. 62401309), and the Qingdao Natural Science Foundation (Project No. 24-4-4-zrjj-89-jch).

REFERENCES

- [1] J. Yao, J. Wang, I. W. Tsang, Y. Zhang, J. Sun, C. Zhang, and R. Zhang, "Deep learning from noisy image labels with quality embedding," *IEEE Transactions on Image Processing*, vol. 28, no. 4, pp. 1909–1922, 2018.

- [2] T. Cour, B. Sapp, and B. Taskar, "Learning from partial labels," *The Journal of Machine Learning Research*, vol. 12, pp. 1501–1536, 2011.
- [3] W. Wang and M.-L. Zhang, "Partial label learning with discrimination augmentation," in *Proceedings of the 28th ACM SIGKDD Conference on Knowledge Discovery and Data Mining*, 2022, pp. 1920–1928.
- [4] J. Song, L. Gao, F. Nie, H. T. Shen, Y. Yan, and N. Sebe, "Optimized graph learning using partial tags and multiple features for image and video annotation," *IEEE Transactions on Image Processing*, vol. 25, no. 11, pp. 4999–5011, 2016.
- [5] W. Hu, Y. Yang, and H. Hu, "Pseudo label association and prototype-based invariant learning for semi-supervised nir-vis face recognition," *IEEE Transactions on Image Processing*, vol. 33, pp. 1448–1463, 2024.
- [6] T. Berg, A. Berg, J. Edwards, and D. Forsyth, "Who's in the picture," *Advances in neural information processing systems*, vol. 17, 2004.
- [7] J. Luo and F. Orabona, "Learning from candidate labeling sets," *Advances in neural information processing systems*, vol. 23, 2010.
- [8] J. Chai, I. W. Tsang, and W. Chen, "Large margin partial label machine," *IEEE Transactions on Neural Networks and Learning Systems*, vol. 31, no. 7, pp. 2594–2608, 2019.
- [9] Y. Yao, J. Deng, X. Chen, C. Gong, J. Wu, and J. Yang, "Deep discriminative cnn with temporal ensembling for ambiguously-labeled image classification," in *Proceedings of the aaai conference on artificial intelligence*, vol. 34, no. 07, 2020, pp. 12 669–12 676.
- [10] Y. Yao, C. Gong, J. Deng, and J. Yang, "Network cooperation with progressive disambiguation for partial label learning," in *Machine Learning and Knowledge Discovery in Databases: European Conference, ECML PKDD 2020, Ghent, Belgium, September 14–18, 2020, Proceedings, Part II*. Springer, 2021, pp. 471–488.
- [11] J. Fan, Y. Yu, Z. Wang, and J. Gu, "Partial label learning based on disambiguation correction net with graph representation," *IEEE Transactions on Circuits and Systems for Video Technology*, vol. 32, no. 8, pp. 4953–4967, 2021.
- [12] J. Ho, A. Jain, and P. Abbeel, "Denoising diffusion probabilistic models," *Advances in neural information processing systems*, vol. 33, pp. 6840–6851, 2020.
- [13] G. Plonka and J. Ma, "Nonlinear regularized reaction-diffusion filters for denoising of images with textures," *IEEE Transactions on Image Processing*, vol. 17, no. 8, pp. 1283–1294, 2008.
- [14] X. Han, H. Zheng, and M. Zhou, "Card: Classification and regression diffusion models," *Advances in Neural Information Processing Systems*, vol. 35, pp. 18 100–18 115, 2022.
- [15] L. Liu and T. Dietterich, "A conditional multinomial mixture model for superset label learning," *Advances in neural information processing systems*, vol. 25, 2012.
- [16] M.-L. Zhang, B.-B. Zhou, and X.-Y. Liu, "Partial label learning via feature-aware disambiguation," in *Proceedings of the 22nd ACM SIGKDD international conference on knowledge discovery and data mining*, 2016, pp. 1335–1344.
- [17] J. Fan, Z. Jiang, Y. Xian, and Z. Wang, "A multi-class partial hinge loss for partial label learning," *Applied Intelligence*, vol. 53, no. 23, pp. 28 333–28 348, 2023.
- [18] J. Fan, Y. Yu, and Z. Wang, "Addressing label ambiguity imbalance in candidate labels: Measures and disambiguation algorithm," *Information Sciences*, vol. 612, pp. 1–19, 2022.
- [19] Y.-C. Chen, V. M. Patel, J. K. Pillai, R. Chellappa, and P. J. Phillips, "Dictionary learning from ambiguously labeled data," in *Proceedings of the IEEE Conference on Computer Vision and Pattern Recognition*, 2013, pp. 353–360.
- [20] J. Fan, Y. Yu, and Z. Wang, "Partial label learning with competitive learning graph neural network," *Engineering Applications of Artificial Intelligence*, vol. 111, p. 104779, 2022.
- [21] J. Lv, M. Xu, L. Feng, G. Niu, X. Geng, and M. Sugiyama, "Progressive identification of true labels for partial-label learning," in *international conference on machine learning*. PMLR, 2020, pp. 6500–6510.
- [22] H. Wen, J. Cui, H. Hang, J. Liu, Y. Wang, and Z. Lin, "Leveraged weighted loss for partial label learning," in *International conference on machine learning*. PMLR, 2021, pp. 11 091–11 100.
- [23] J. Fan, Y. Yu, L. Huang, and Z. Wang, "Graphdipi: Partial label disambiguation by graph representation learning via mutual information maximization," *Pattern Recognition*, vol. 134, p. 109133, 2023.
- [24] H. Wang, R. Xiao, Y. Li, L. Feng, G. Niu, G. Chen, and J. Zhao, "Pico+: Contrastive label disambiguation for robust partial label learning," *IEEE Transactions on Pattern Analysis and Machine Intelligence*, 2023.
- [25] J. Fan, L. Huang, C. Gong, Y. You, M. Gan, and Z. Wang, "Kmt-pll: K-means cross-attention transformer for partial label learning," *IEEE Transactions on Neural Networks and Learning Systems*, 2024.
- [26] N. Xu, C. Qiao, X. Geng, and M.-L. Zhang, "Instance-dependent partial label learning," *Advances in Neural Information Processing Systems*, vol. 34, pp. 27 119–27 130, 2021.
- [27] N. Xu, C. Qiao, Y. Zhao, X. Geng, and M.-L. Zhang, "Variational label enhancement for instance-dependent partial label learning," *IEEE Transactions on Pattern Analysis and Machine Intelligence*, 2024.
- [28] S. Xia, J. Lv, N. Xu, and X. Geng, "Ambiguity-induced contrastive learning for instance-dependent partial label learning," in *IJCAI*, 2022, pp. 3615–3621.
- [29] D.-D. Wu, D.-B. Wang, and M.-L. Zhang, "Distilling reliable knowledge for instance-dependent partial label learning," in *Proceedings of the AAAI Conference on Artificial Intelligence*, vol. 38, no. 14, 2024, pp. 15 888–15 896.
- [30] J. Yue, L. Fang, S. Xia, Y. Deng, and J. Ma, "Dif-fusion: Toward high color fidelity in infrared and visible image fusion with diffusion models," *IEEE Transactions on Image Processing*, vol. 32, pp. 5705–5720, 2023.
- [31] D. P. Kingma, "Auto-encoding variational bayes," *arXiv preprint arXiv:1312.6114*, 2013.
- [32] I. Goodfellow, J. Pouget-Abadie, M. Mirza, B. Xu, D. Warde-Farley, S. Ozair, A. Courville, and Y. Bengio, "Generative adversarial networks," *Communications of the ACM*, vol. 63, no. 11, pp. 139–144, 2020.
- [33] J. Song, C. Meng, and S. Ermon, "Denoising diffusion implicit models," *arXiv preprint arXiv:2010.02502*, 2020.
- [34] J. Chen, R. Zhang, T. Yu, R. Sharma, Z. Xu, T. Sun, and C. Chen, "Label-retrieval-augmented diffusion models for learning from noisy labels," *Advances in Neural Information Processing Systems*, vol. 36, 2024.
- [35] K. Pandey, A. Mukherjee, P. Rai, and A. Kumar, "Diffusevae: Efficient, controllable and high-fidelity generation from low-dimensional latents," *arXiv preprint arXiv:2201.00308*, 2022.
- [36] F. Briggs, X. Z. Fern, and R. Raich, "Rank-loss support instance machines for m1ml instance annotation," in *Proceedings of the 18th ACM SIGKDD international conference on Knowledge discovery and data mining*, 2012, pp. 534–542.
- [37] Z. Zeng, S. Xiao, K. Jia, T.-H. Chan, S. Gao, D. Xu, and Y. Ma, "Learning by associating ambiguously labeled images," in *Proceedings of the IEEE Conference on computer vision and pattern recognition*, 2013, pp. 708–715.
- [38] M. Guillaumin, J. Verbeek, and C. Schmid, "Multiple instance metric learning from automatically labeled bags of faces," in *Computer Vision—ECCV 2010: 11th European Conference on Computer Vision, Heraklion, Crete, Greece, September 5–11, 2010, Proceedings, Part I 11*. Springer, 2010, pp. 634–647.
- [39] Y. LeCun, L. Bottou, Y. Bengio, and P. Haffner, "Gradient-based learning applied to document recognition," *Proceedings of the IEEE*, vol. 86, no. 11, pp. 2278–2324, 1998.
- [40] T. Clanuwat, M. Bober-Irizar, A. Kitamoto, A. Lamb, K. Yamamoto, and D. Ha, "Deep learning for classical japanese literature," *arXiv preprint arXiv:1812.01718*, 2018.
- [41] A. Krizhevsky, G. Hinton *et al.*, "Learning multiple layers of features from tiny images," 2009.
- [42] H. Xiao, K. Rasul, and R. Vollgraf, "Fashion-mnist: a novel image dataset for benchmarking machine learning algorithms," *arXiv preprint arXiv:1708.07747*, 2017.
- [43] F. Zhang, L. Feng, B. Han, T. Liu, G. Niu, T. Qin, and M. Sugiyama, "Exploiting class activation value for partial-label learning," in *International conference on learning representations*, 2021.
- [44] D.-D. Wu, D.-B. Wang, and M.-L. Zhang, "Revisiting consistency regularization for deep partial label learning," in *International conference on machine learning*. PMLR, 2022, pp. 24 212–24 225.
- [45] T. Chen, S. Kornblith, M. Norouzi, and G. Hinton, "A simple framework for contrastive learning of visual representations," in *International conference on machine learning*. PMLR, 2020, pp. 1597–1607.
- [46] A. Radford, J. W. Kim, C. Hallacy, A. Ramesh, G. Goh, S. Agarwal, G. Sastry, A. Askell, P. Mishkin, J. Clark *et al.*, "Learning transferable visual models from natural language supervision," in *International conference on machine learning*. PMLR, 2021, pp. 8748–8763.
- [47] D. Hendrycks, K. Lee, and M. Mazeika, "Using pre-training can improve model robustness and uncertainty," in *International conference on machine learning*. PMLR, 2019, pp. 2712–2721.
- [48] C. Guo, G. Pleiss, Y. Sun, and K. Q. Weinberger, "On calibration of modern neural networks," in *International conference on machine learning*. PMLR, 2017, pp. 1321–1330.